16.512, Rocket Propulsion
Prof. Manuel Martinez-Sanchez
Lecture 26: Turbopumps

Turbopump Components

The mechanical components of the pressurization cycle (pumps and turbines) are next to be considered. An excellent recent survey of this area is given in Ref.40. A more comprehensive, but older survey is contained in a series of NASA SP reports [41-43]. Pumps and turbines will first be discussed separately, and their integration will then be examined.

(a) Pumps

Almost all existing rockets have centrifugal turbopumps. These deliver more ΔP per stage than axial flow pumps, with only slightly less efficiency. Only if multistaging becomes necessary is there a possible incentive to go to axial pumps; this happens with LH_2 fuel, where, due to the low density, the ΔP per stage is limited by the attainable rim speeds.

In general, the design attempts to maximize operating speed, since this reduces the pump size, and hence the weight. Pump speed is limited by several effects, most importantly cavitation at inlet. Others are centrifugal stresses (either at the impeller or in the driving turbine), limiting peripheral speeds for bearing and seals, and avoidance of critical speeds.

"Head rise" is used commonly instead of pressure rise to express the performance of pumps. We can define head rise as the height to which one could raise one Kg of fluid with the amount of ideal work per Kg done by the pump:

$$H = \Delta h_s / g = \int_{P_1}^{P_2} \frac{dp}{\rho g} \tag{1}$$

The rise is directly related to the pump work, even if the fluid has significant compressibility:

$$\text{Work/mass} = \Delta h = \frac{gH}{\eta_p} \tag{2}$$

and this is one of the advantages of its use. Obviously, if ρ = const.,

$$H = \frac{\Delta P}{\rho g}, \qquad \frac{\text{Work}}{\text{mass}} = \frac{\Delta P}{\rho\, \eta_p} \tag{3}$$

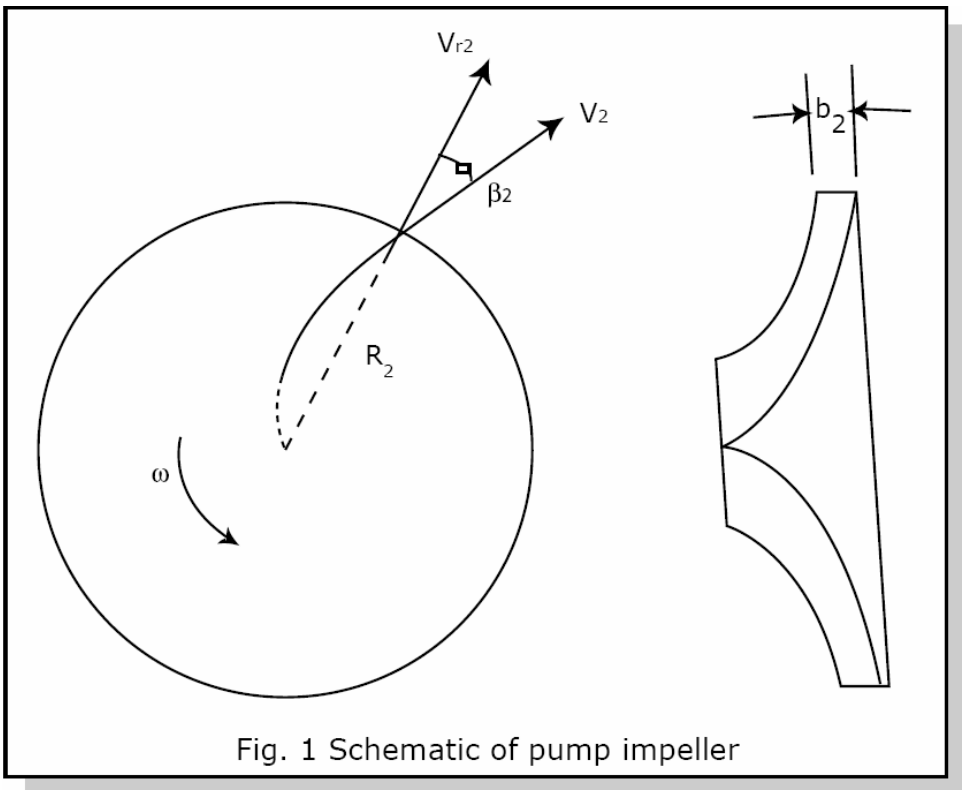

Fig. 1 Schematic of pump impeller

The head rise is directly to the peripheral speed of the impeller disk. The fluid enters axially near they impeller hub, with no angular momentum; it leaves the impeller with absolute tangential speed $\omega R_2 - V_{r2} \tan \beta_2$, where β_2 is the back-leaning blade angle at the rim Fig 1, and V_{r2} is the fluid radial exit velocity, related to the volume flow rate as

$$Q = 2\pi R_2 b_2 V_{r2} \tag{4}$$

The torque needed to drive the impeller is the net outflow rate of angular momentum, and the work rate is this, times ω. Thus,

$$\text{Power} = \dot{m}(\omega R_2)^2 \left(1 - \frac{V_{r2}}{\omega R_2} \tan \beta_2\right) \tag{5}$$

and since we also have $\text{Power} = \dot{m} \frac{gH}{\eta_p}$, the head rise is

$$H = \eta_p \frac{(\omega R_2)^2}{g} \left(1 - \frac{V_{r2}}{\omega R_2} \tan \beta_2\right) \tag{6}$$

The quantity $\psi = \eta_p \left(1 - \frac{V_{r2}}{\omega R_2} \tan \beta_2 \right)$ is sometimes called the "head coefficient." In terms of ψ,

$$H = \psi \frac{(\omega R_2)^2}{g} \tag{7}$$

ψ is typically between 0.2 and 0.8. Values greater than unity could be obtained if the blades were designed to learn <u>forward</u> ($\beta_2 < 0$), but then ΔP would increase with Q (through the effect of V_{r2}). This positive slope of the ΔP vs. Q characteristic is known to produce instabilities in the pumping system [44]. These are generally dynamic in nature, and depend to some extent on the characteristics of the rest of the system (free volume, throttling effects, etc), but it is relatively easy to understand their origin from a quasistatic argument: if the pump temporarily delivers more flow than can be disposed of in steady state by the downstream components, and if its characteristic has a positive slope $\frac{\partial(\Delta P)}{\partial Q}$, the pump pressure rise will also be higher than normal. The downstream pressure will therefore tend to increase for <u>both reasons</u>, and a runaway situation ensues. In addition to this system instability, there is also a tendency for flow maldistribution analogous to rotating stall, since the flow is then unstable with respect to mass interchange between parallel streamtubes [45].

Eq. (6) would predict a <u>linear</u> dependence of head on flow rate. In reality varying the flow at a given speed will vary the internal flow angles with respect to blades, and will therefore result in variations of the slope $\partial H / \partial Q$. Examples of this behavior are shown in Fig 2 (Ref. 41), where the flow coefficient is defined as

$$\varnothing_2 = \frac{Q}{2\pi R_2 b_2 (\omega R_2)} \tag{8}$$

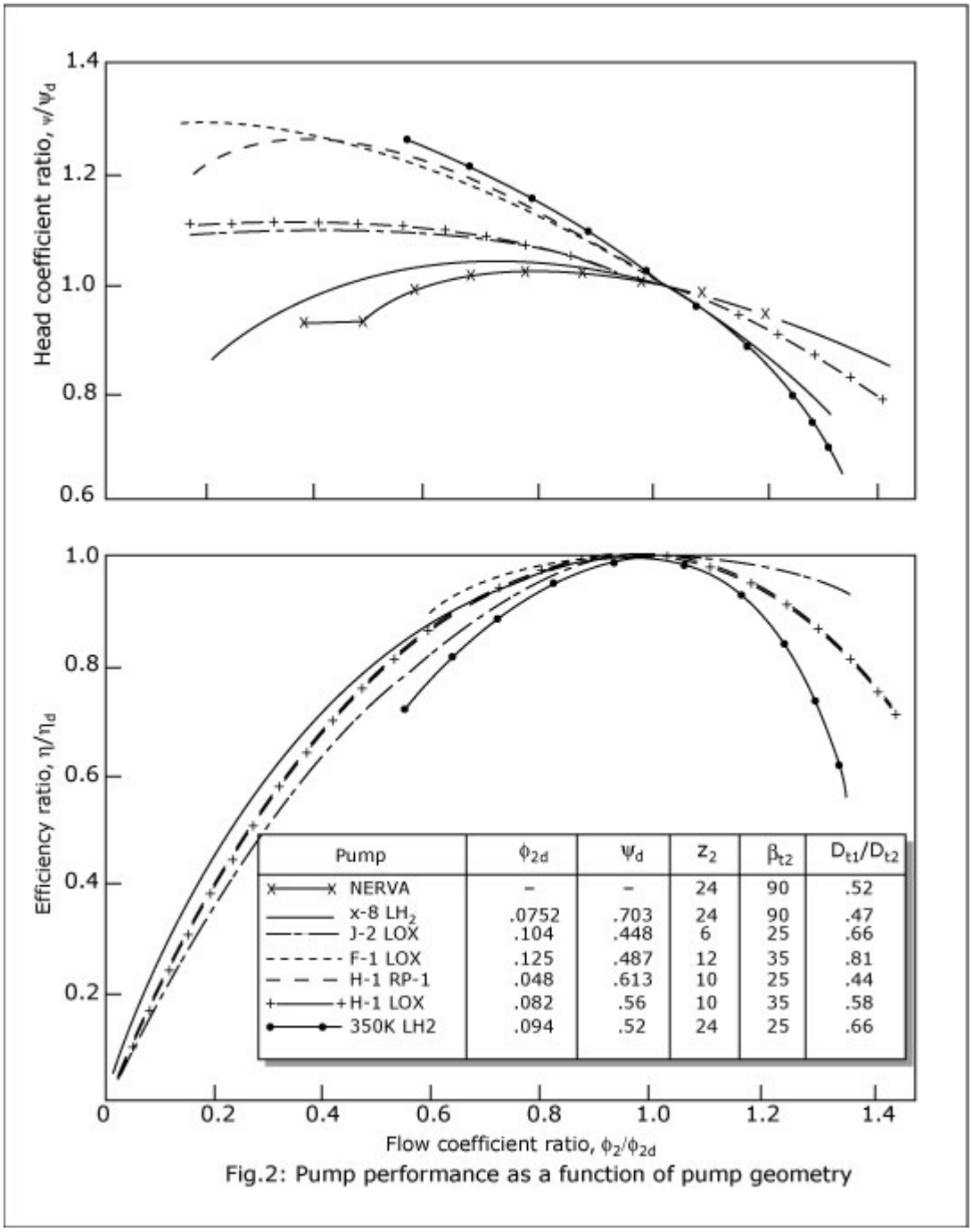

Fig.2: Pump performance as a function of pump geometry

The throttling range is defined by the point of maximum head, below which operation is unstable. Similar (but stronger) restrictions apply to axial designs, such as that used in the J-2 LH pump, and so these designs tend to be limited to applications which require very limited throttling.

The pump is designed to specified head rise H or (ΔP) and volumetric flow Q. These quantities can be used to construct the non dimensional quantities called specific diameter and specific speed:

$$d_s = \frac{D(gH)^{1/4}}{Q^{1/2}} \tag{9}$$

$$n_s = \frac{\omega Q^{1/2}}{(gH)^{3/4}} \tag{10}$$

In the U.S. literature, D is expressed in feet, Q in gpm and ω in rpm, and g is omitted. This procedure, of questionable practically, result in related parameters D_s, N_s given By N_s= 2728 n_s, Ds = 0.01985d_s.

Notice that

$$n_s d_s = \frac{\omega D}{(gH)^{1/2}} \tag{11}$$

and hence, from (7),

$$n_s d_s = \frac{2}{\sqrt{\psi}} \tag{12}$$

or, in English units, $N_s D_s = 108.3/\sqrt{\psi}$. Since for centrifugal pumps, we found ψ <1, we can see that their domain is a (n_s, d_s) map is $n_s d_s$ >2 (or $N_s D_s > 108$).

The considerable empirical evidence on pump performance has been distilled (Ref.46) by constructing (n_s, d_s) maps on which favorable regions are shown for various types of machine. A very generalized example (taken from Ref. 41) is shown in Fig. 3, where lines of constant peak efficiency are shown for a wide variety of pumps. These use a set of clearance, tolerance, roughness, etc. factors, and are to be taken only as indicative, since actual design may depart from adopted values. We notice in Fig. 3 the line $N_s D_s \sim 100$, denoted as the "limit for dynamic pumps", in accordance to our discussion above. Radial and axial pump designs nearly merge, although the axial type is indicated for the highest specific speed, which as Eq. 10 shows, may be simply a reflection of low head rise, as for example, in the inducer stages featured commonly at the inlet of centrifugal pumps for cavitation suppression. Table 1 gives the features of the high pressure SSME pumps, and the resulting (N_s, D_s) points are included in Fig 3, where they are seen to lie roughly on the η = 0.8 line.

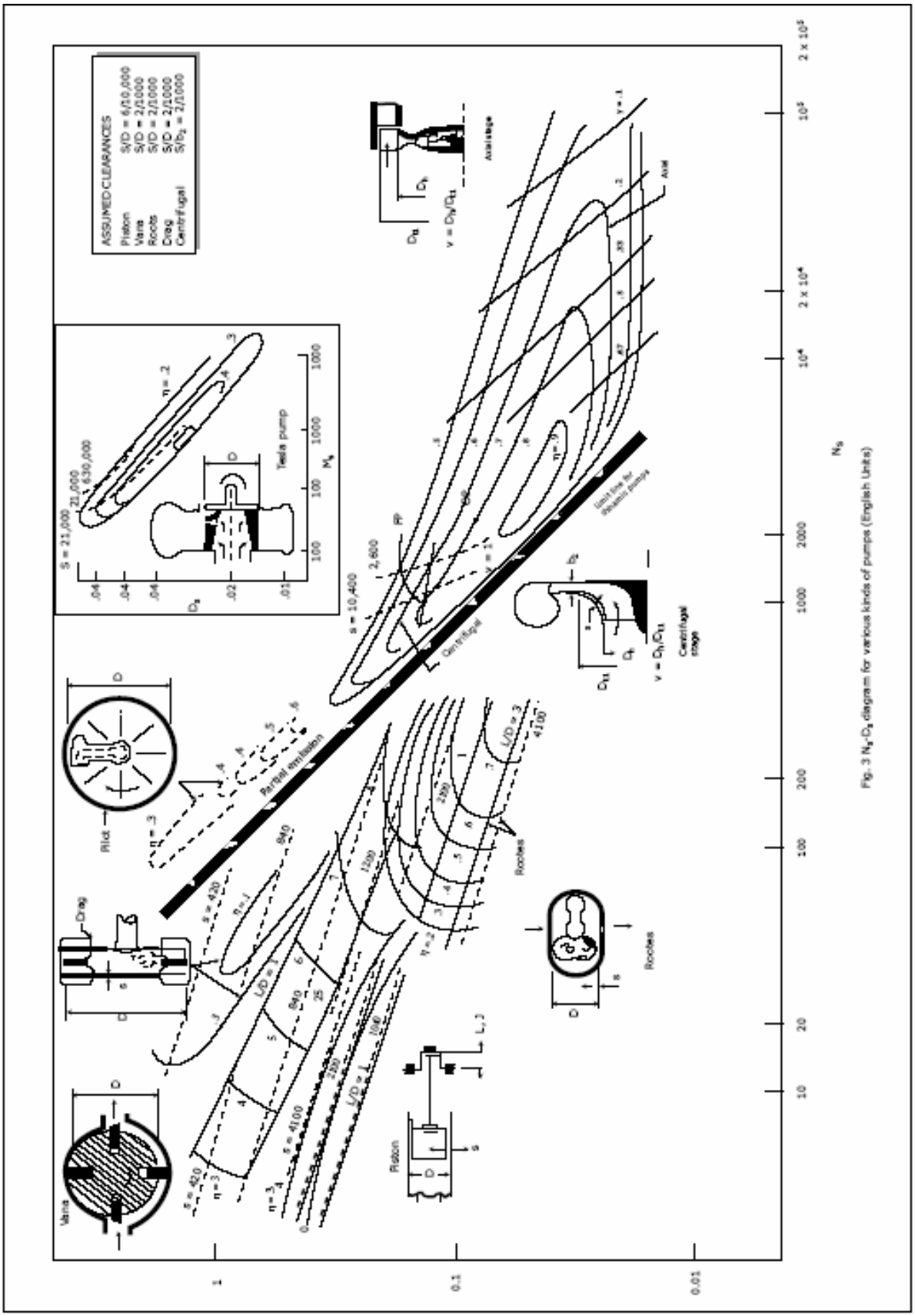

Fig. 3 N_s-D_s diagram for various kinds of pumps (English Units)

The pumps must be designed so as to avoid cavitation, which both, degrades performance, and causes damage to reusable articles. Cavitation risk exists at the pump inlet, where the liquid pressure is lowest, and it increases with both, the fluid velocity and the speed of the pump inducer blades meeting the fluid. The inducer diameter needs to be large enough to reduce the inlet fluid dynamic head $\frac{1}{2}\rho C_m^2$ to some fraction of the excess inlet pressure over saturation P_1-$P_{sat,\ 1}$. This last quantity is called the Net Positive Suction Pressure (NPSP), and is usually given as a suction head NPSH= NPS/(ρg).

	Hydrogen Pump	Oxygen Pump
ΔP (N/m^2)	1.38×10^7 (per stage)	3.30×10^7
H (m)	20,000	2,930
Q (m^3/sec)	0.96	0.229 (per side)
ω (rad/sec)	3674	3246
D (m)	0.308	0.16
n_s (N_s)	0.386 (1050)	0.703 (1920)
d_s (D_s)	6.61 (0.0131)	435 (0.0866)

Table 1. Characteristics of the SSME high-pressure fuel and oxidizer pumps

The ratio:

$$\sigma = \frac{(NPSP)}{\frac{1}{2}\rho C_m^2} = \frac{(NPSP)}{C_m^2/2g} \tag{13}$$

is called the Thoma parameter, and empirical evidence [40,41] indicates that it should be grater than 1 for LH, 2 for LOX and 3 for water and storable propellants. The more favorable situation for hydrogen appears to be related to a greater vapor suppression effect due to evaporate chilling when bubbles start to form.

Several other parametric representations of cavitation data exist. Thus, Refs [40] and [41] use a "suction specific speed" S_s defined as in Eq (10), but with H replaced by the NPSH, and with correction for flow blockage by the hub. This parameter can be shown to be related to Thoma's parameter σ and to $\varnothing_t = c_m / \omega R_1$ (R_1= inducer radius) by

$$S_s = \frac{2.981}{\sigma^{3/4}\varnothing_t} \tag{14}$$

In English units, the numerical factor is 8132. The data on cavitations onset for a variety of liquids show that σ remains approximately constant for each, as noted above. Independently, Ref. 47 shows cavitations results in the form

$$\tau = f(Z_t) \tag{15}$$

where

$$\tau = \frac{NPSP}{\frac{1}{2}\rho\left(\omega R_1\right)^2} \quad ; \quad Z_t = \frac{\sin\vartheta}{1+\cos\vartheta}\,\varnothing_t \tag{16}$$

and ϑ is the inducer leading edge blade angle, which, at design conditions, is close to $\tan^{-1}\varnothing_t$ and is typically $5^0 - 10^0$. The data lies close to the line $\tau = 3Z_t$. With small angle approximations for ϑ and $\varnothing_t$, this can be shown to be equivalent to $\sigma = 3/2$, intermediate between Stangeland's recommendations [40] for LH and LOX.

With the inducer diameter chosen from the above criteria, the shaft speed is limited [40] so as to keep the inducer tip speed below 170 m/sec (LOX) or 340 m/sec (LH). This is done in order to control cavitation in the blade-tip leakage vortex [40]. This speed limitation may conflict with the desire to place the (r_s, d_s) point on a favorable spot in the efficiency maps. In that case, the NPSH must be raised, either by partial pressurization of the tanks, or, as in the SSME, by the use of separate low-pressure booster pumps. These are only rough guidelines, and, the precise allowable limits depend upon detailed design of the inducer. Progress in inducer design has been a pacing item in allowing turbopump speed to increase, thus reducing weight (as well as increasing life).

References cited:

40. M. L. Joe Stangeland. "*Turbopumps for Liquid Rockets Engines*". Ninth Cliff Garrett Turbomachinery' Award Lecture, April 7, 1992. SAE/SP-92/924.

41. Turbopump Systems for Liquid Rocket Engines, NASA SP-8107, Aug. 1974.

42. Liquid Rocket Engine Turbines, NASA SP-8110, Jan 1974.

43. Liquid Rocket Engines Centrifugal Flow Turbopumps, NASA SP-8109, Dec. 1973.

44. E.M. Greitzer, "*The Stability of Pumping Systems*", ASME, Transactions, Jl. of Fluids Engineering 103 (1981), pp.193-242.

45. J.L.Kerrebrock, Aircraft Engines and Gas Turbines, MIT press. 1992 (Sec.5-7).

46. O.E. Balje, Turbomachines: A Guide to Design, Selection and Theory, J. Wiley & Sons, New York, 1981.

47. L.B. Stripling, "*Cavitation in Turbopumps*", pt. 2, Trans. ASME, Series D, J. Of Basic Engineering (1962): 339.